

Three-Dimensional Finite Element Analysis of a Reinforced Paved Road

G. Dondi
Bologna University, Italy

ABSTRACT: The main objective of this work is to determine the behaviour of a paved road reinforced with geosynthetics placed at the bottom of the road foundation. The subgrade is of cohesive soil which is shown to benefit from the interposition of geosynthetics.

Analysis presented in this paper demonstrates that the friction developed between the geosynthetic and the granular soil in the foundation layer considerably reduces the shear stress between the geosynthetics and the subsoil. This effect seems to give increased life to the pavement.

1. INTRODUCTION

The first documented experiences of reinforcing temporary road with geosynthetics (fig. 1) date from the 1970s (Hausmann, 1987; Dondi and Righi, 1990). Thereafter, applications were extended to include paved roads (Chan et al., 1989, Miura et al., 1988).

Contrary to the above, there has not been the same development of calculating methods for paved roads in the presence of soft cohesive soils (CBR < 2-3 %) that make it possible to quantify the consequences due to inserting geosynthetic reinforcements between the layers, in terms of stresses and strains. The methods that have been developed thus far consider the reinforcement based on its characteristics of permeability and weave, and not the strenght it can offer. This is probably due to the scarce knowledge of the mechanism with which this reinforcement is developed.

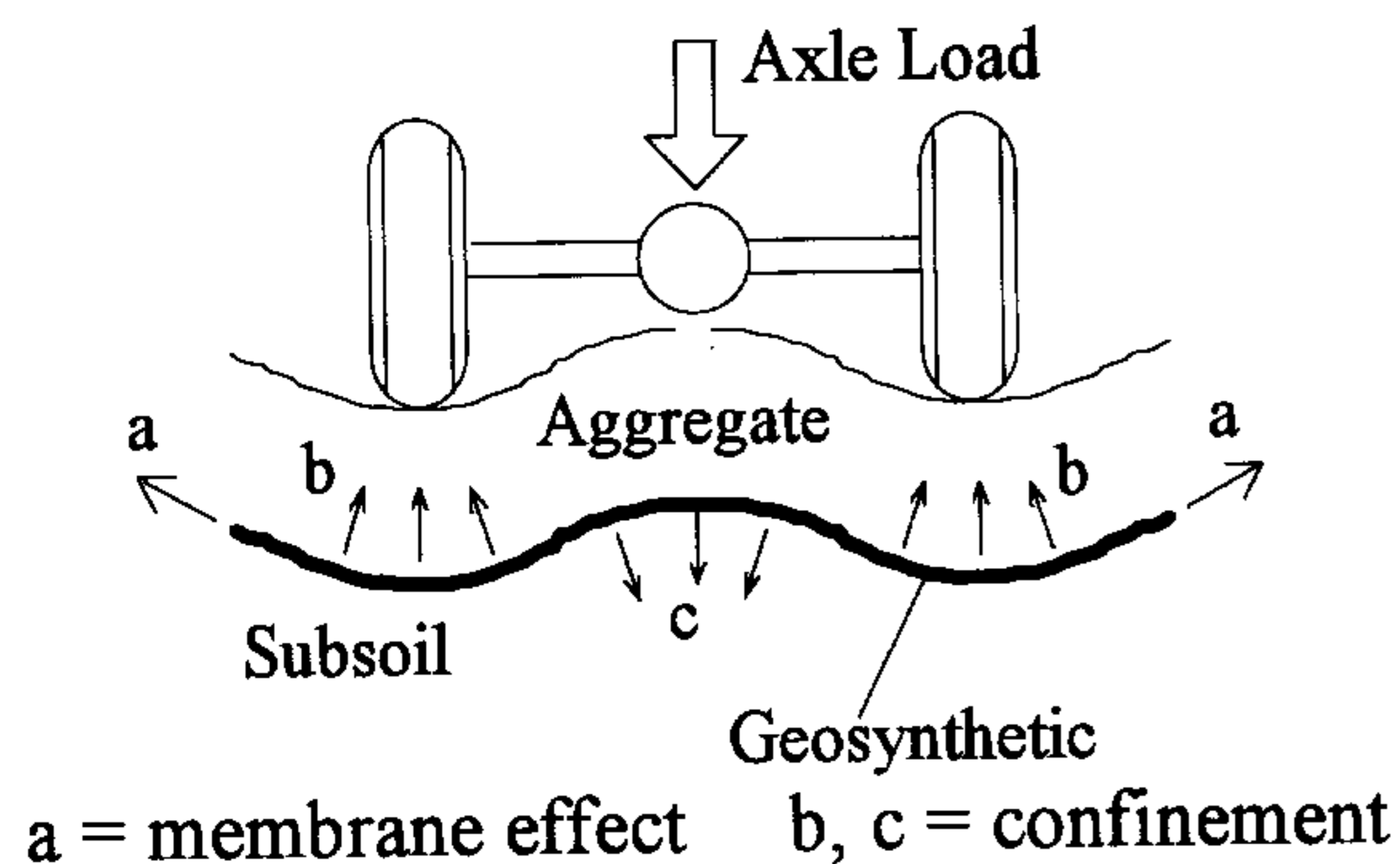


Fig. 1 Reinforcement mechanism in unpaved roads

The substantial difference between temporary and permanent roads may be summarized as follows: while in the former, the appearance of considerable permanent displacements is allowed (even 0.1-0.2 m), this is 'nt acceptable in the latter.

Most of the methods proposed by various authors regarding temporary roads take into account the membrane effect (see Fig. 1) as a reinforcing action, hypothesizing the existence of significant permanent displacements (Barenberg, 1980; Giroud and Noiray, 1981; Sellmeier et al., 1982).

On paved roads, the hypotheses for this type of procedure are not admissible, and it is fair to imagine that the improvements due to the presence of geosynthetics, undoubtedly found in practice, are due to the mentioned membrane behaviour of the latter, which would require the presence of vertical displacements greater than 0.1 m (Giroud et al., 1984). It is more logical instead to think that the reinforcement function is carried out due to absorption by means of the geosynthetic, which therefore goes in tension, of the shear stress that would otherwise be transmitted to the soil (Houlsby and Jewell, 1990), thus actually causing a decrease in the entity of the shearing components of stresses and strains on the sub-soil (see Fig. 2).

In current design methods for paved roads (Christopher and Holtz, 1991), the geosynthetic is taken into account only for the separation function and limiting the cracks propagation, not including the possibility of reducing the thickness of the layers.

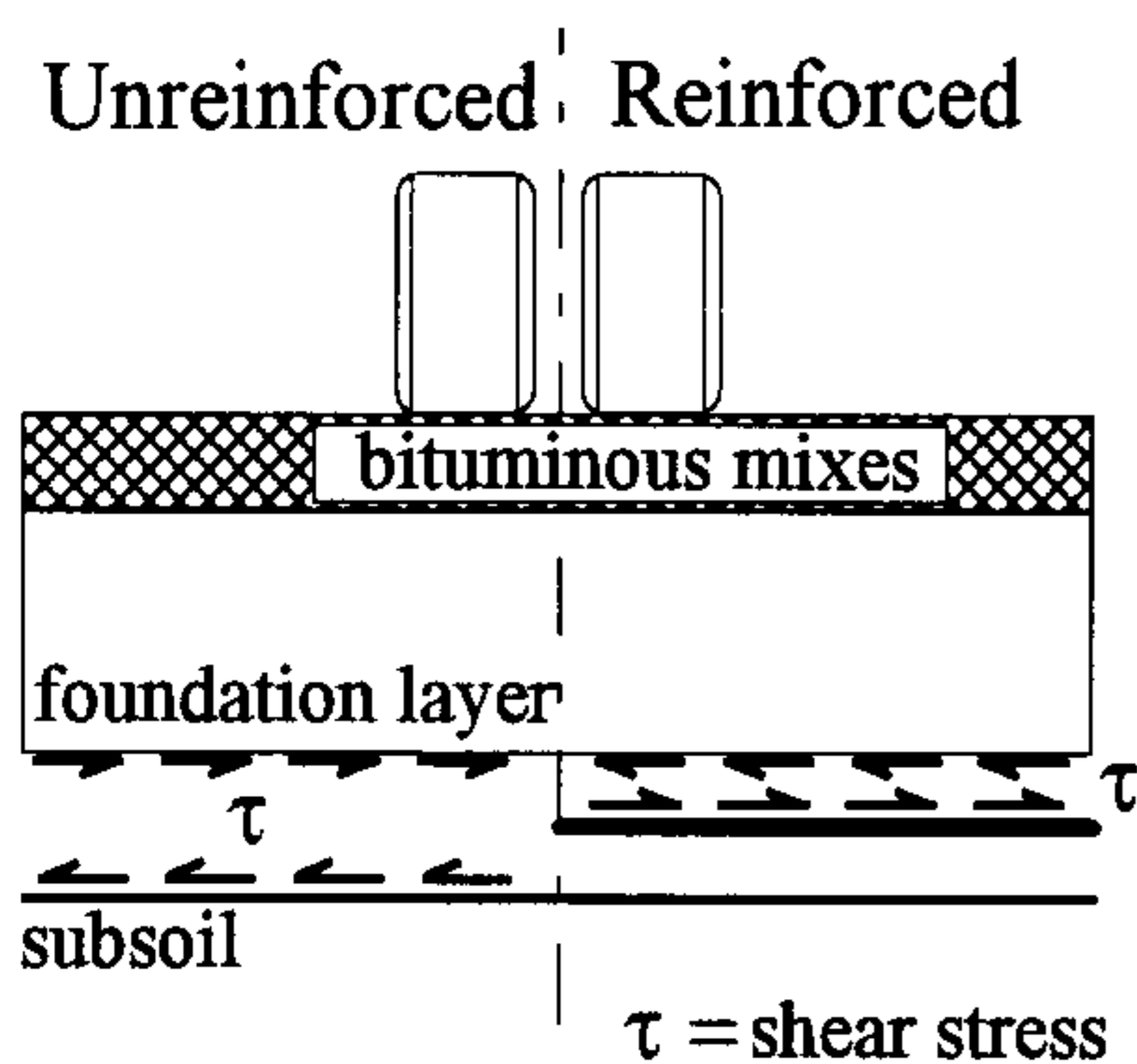


Fig. 2 Reinforcement mechanism in paved road

The analytical difficulties related to the study of a reinforced elasto-plastic multilayer, such as that of a road pavement, make it impossible to determine a closed analytical solution. It was thus deemed appropriate to take an approach aimed at discretizing the problem using the Finite Element technique, already used for roads in the plane strain analysis (Burd and Brocklehurst, 1990) and in axial-symmetry (Zeevaert-Wolff, 1982).

2 MATERIALS PROPERTIES

The non-linear constitutive laws of the multilayer materials was simulated by the appropriate models, taking into account the frictional behaviour on the geotextile-soil interface surfaces, in particular, the Cam-Clay model was used (Scofield and Wroth, 1968; Roscoe and Burland, 1968) as far as the cohesive subsoil layer is concerned, and the non-associated Drucker-Prager model (Drucker and Prager, 1952) was employed for the cohesionless foundation layer (see Table 1 for parameters).

Table 1. Constitutive Models and their parameters

Layer	Constitutive model	Parameters
Bituminous mixes	Elastic	$E = 2000 \text{ MPa}$; $\nu = 0.33$.
Foundation	Drucker-Prager	$E = 150 \text{ MPa}$; $\nu = 0.40$; $\phi = 40^\circ$; $\psi = 0^\circ$; $c = 66 \text{ kPa}$.
Geosynthetic	Elastic	$J = 600\text{-}1200 \text{ kN/m}$; $\nu = 0.1$.
Subsoil	Cam-Clay	$k = 0.036$; $\lambda = 0.253$; $M = 0.984$; $e_1 = 2.422$; $\nu = 0.30$.

The table 1 shows the constitutive laws used in the F.E. model and the related parameters. The cohesion in the foundation layer has been introduced only for computational features because the lack of this property can determine the failure of the aggregate layer at the beginning of analysis.

The contact between the geosynthetic-layer surfaces was simulated by means of a Mohr Coulomb-type elastoplastic model.

The following friction coefficients were adopted: $\mu = 0.33$ for contact between the geosynthetic and the cohesive soil; $\mu = 0.56$ for contact between the geosynthetic and the foundation layer.

3. FINITE ELEMENT MODEL

The geometry performance was studied, in the early stages, with a linear elastic material (Chinni, 1992), considering, as the term of comparison, the closed solution, relative to a semi-unlimited elastic multilayer, provided by the BISAR code (De Jong et al., 1973). The choice to operate in a three-dimensional field, justified by the low reliability of two-dimensional models (plane strain), gave appreciable results in the elastic field.

The geometric model used represents a multilayer system reinforced by inserting a geosynthetic at the base of the foundation layer as shown in figure 3.

The load is produced by the passage of a dual-wheel axis; considering a load produced by a single pair of twin wheels led to the presence of two symmetry planes. The mesh was thus conceived so as to limit the number of nodes and elements as highlighted by their arrangement on the horizontal plane.

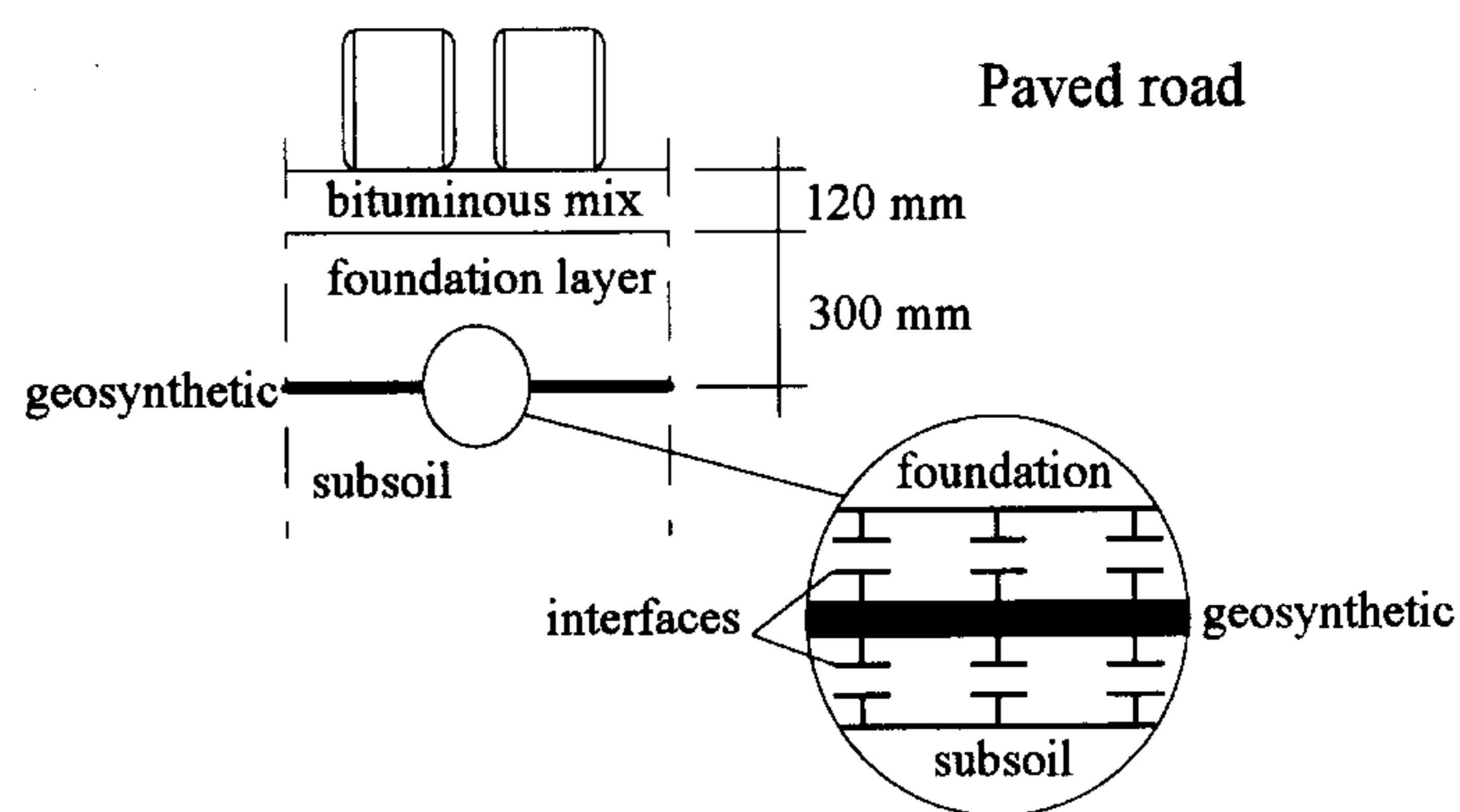


Fig. 3. Composition of the multilayer and schematically representation of the use of interface elements

The geosynthetic was modelled using membrane elements, while the friction that develops on the contact surfaces between the geosynthetic and the layers was simulated by using interface elements with 4 integration

points (Fig. 4). The function of these elements is essential in reproducing a layer with elastoplastic behaviour which still allows mutual reinforcement-soil slippage. In the analyses carried out, it was found that a lack of such elements leads to entirely unreliable results.

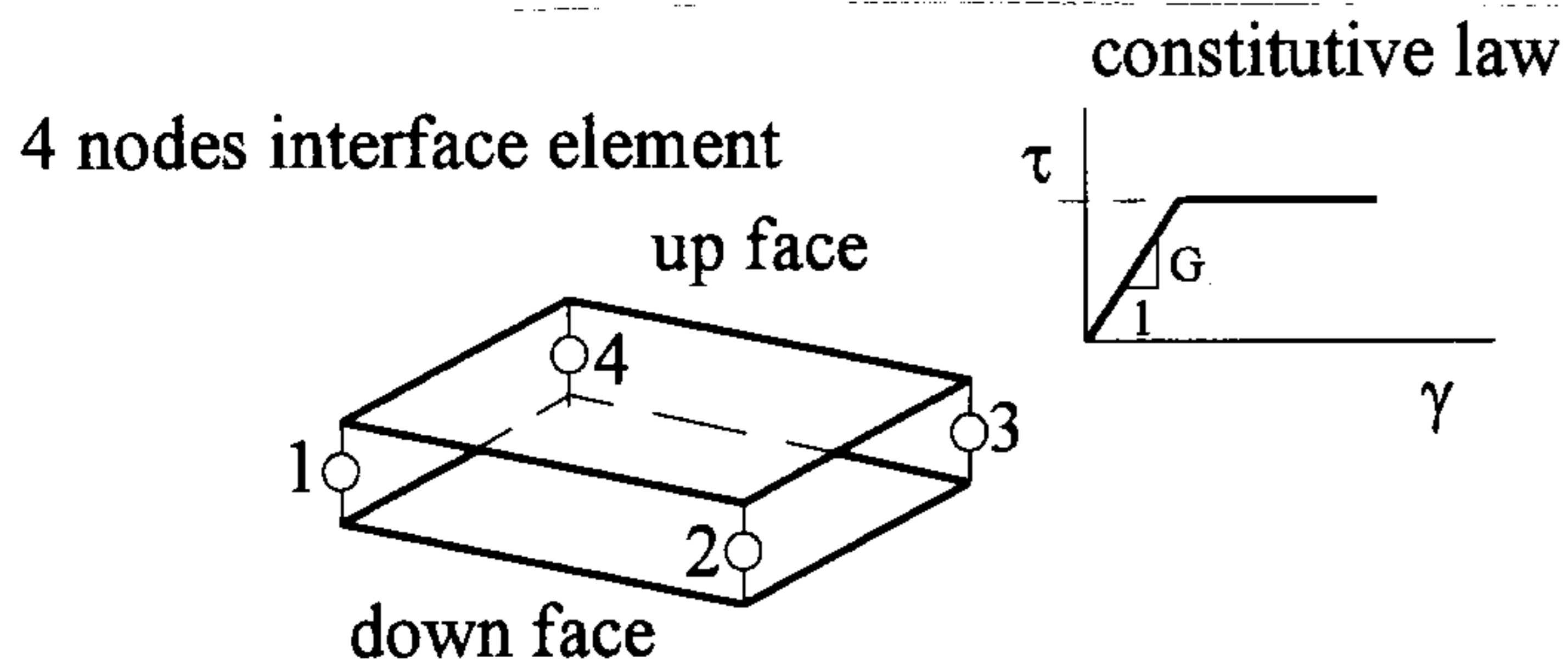


Fig. 4. Four nodes interface element to simulate contact between hexahedral elements and their constitutive law.

The mesh used, with dimensions 2.80 m x 2.80 m on the plane and 2.92 m high (see Fig. 5) is made up, if the reinforcement is present, of 5904 nodes and 5346 elements, divided as follows:

4455 continuous hexahedral elements with 8 nodes and linear deformation (ABAQUS code C3D8) to make up the layers of bituminous concrete, foundation and subsoil; 297 quadrilateral membrane elements with 4 nodes and linear deformation (ABAQUS code M3D4) to make up the layer of geosynthetic; 594 interface elements with 4 integration points (ABAQUS code INTER4) to simulate the elastoplastic contact point between geosynthetic and layers.

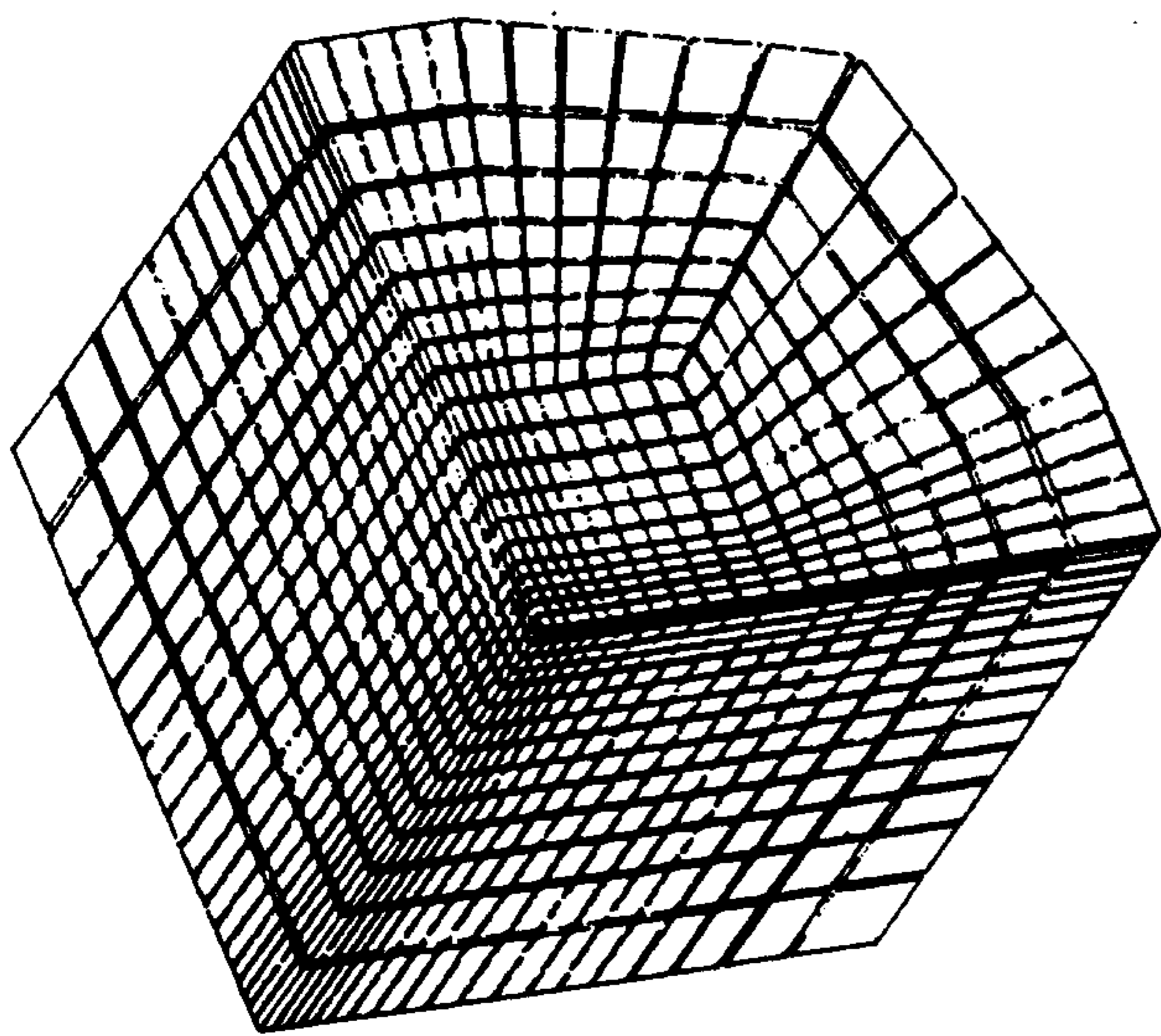


Fig. 5 Mesh of finite-element model

4 RESULTS OF THE ANALYSIS

In this section we consider the paved road behaviour with a load four times higher of this used in the design of Italian motorways (130 kN axle load).

The analysis pointed out that the insertion of a geosynthetic offers a general benefit to the paved road, as shown in the graphs below which describe the pattern of the stress and strain as the load increased. After a preliminary examination of the results, the most stressed elements were identified, and the tension and strain path of these were studied.

Figure 6 shows the verification points for the layers making up the overstructure, in addition to the size of the load area of a pair of wheels used in the model.

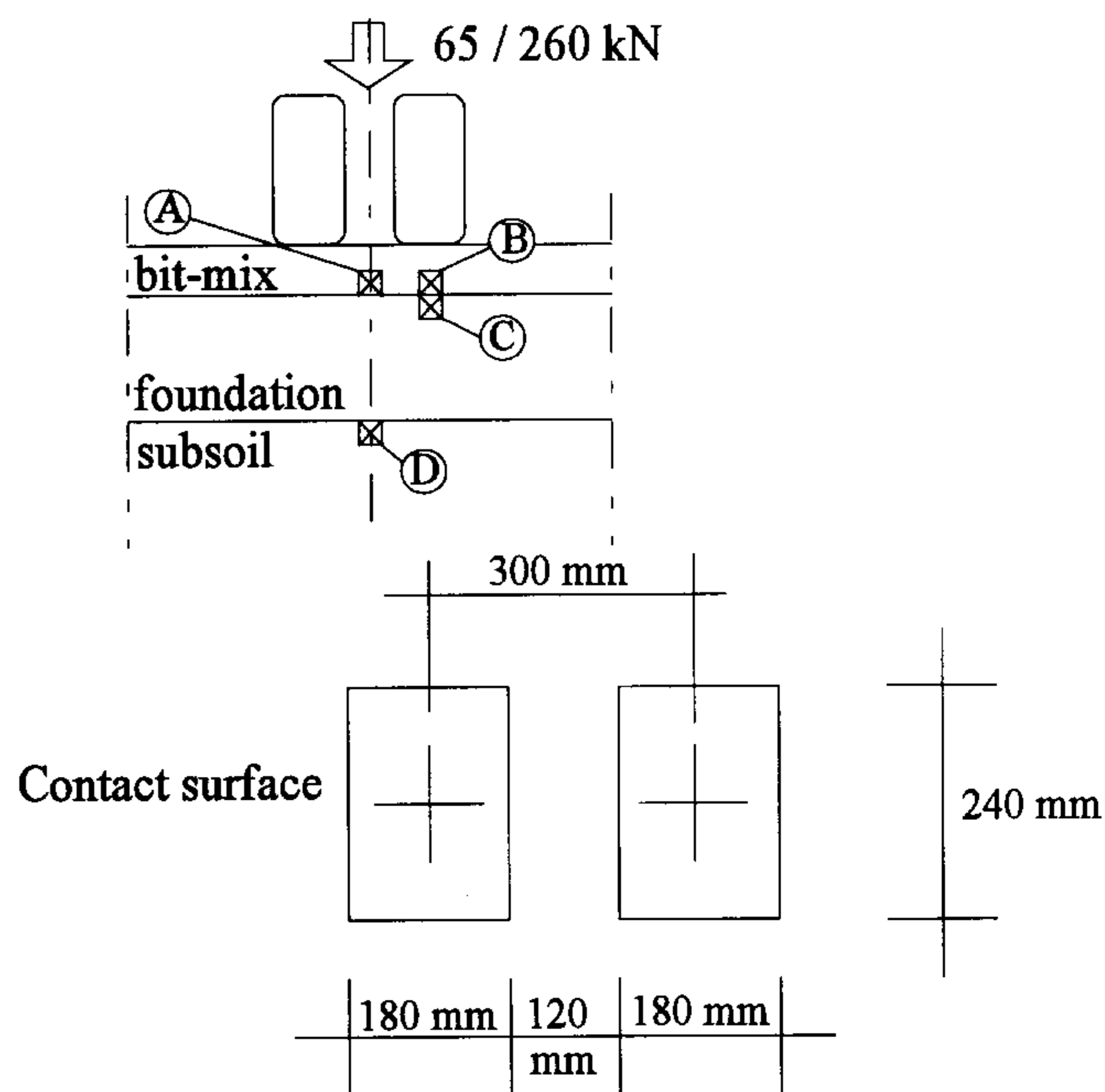


Fig. 6

The strain path of point C, belonging to the aggregate layer, is shown in the graph in figure 7; the total absence of volume strain components after yielding is evident, in accordance with the assumption of a non-associated Drucker-Pager model (dilatancy = 0).

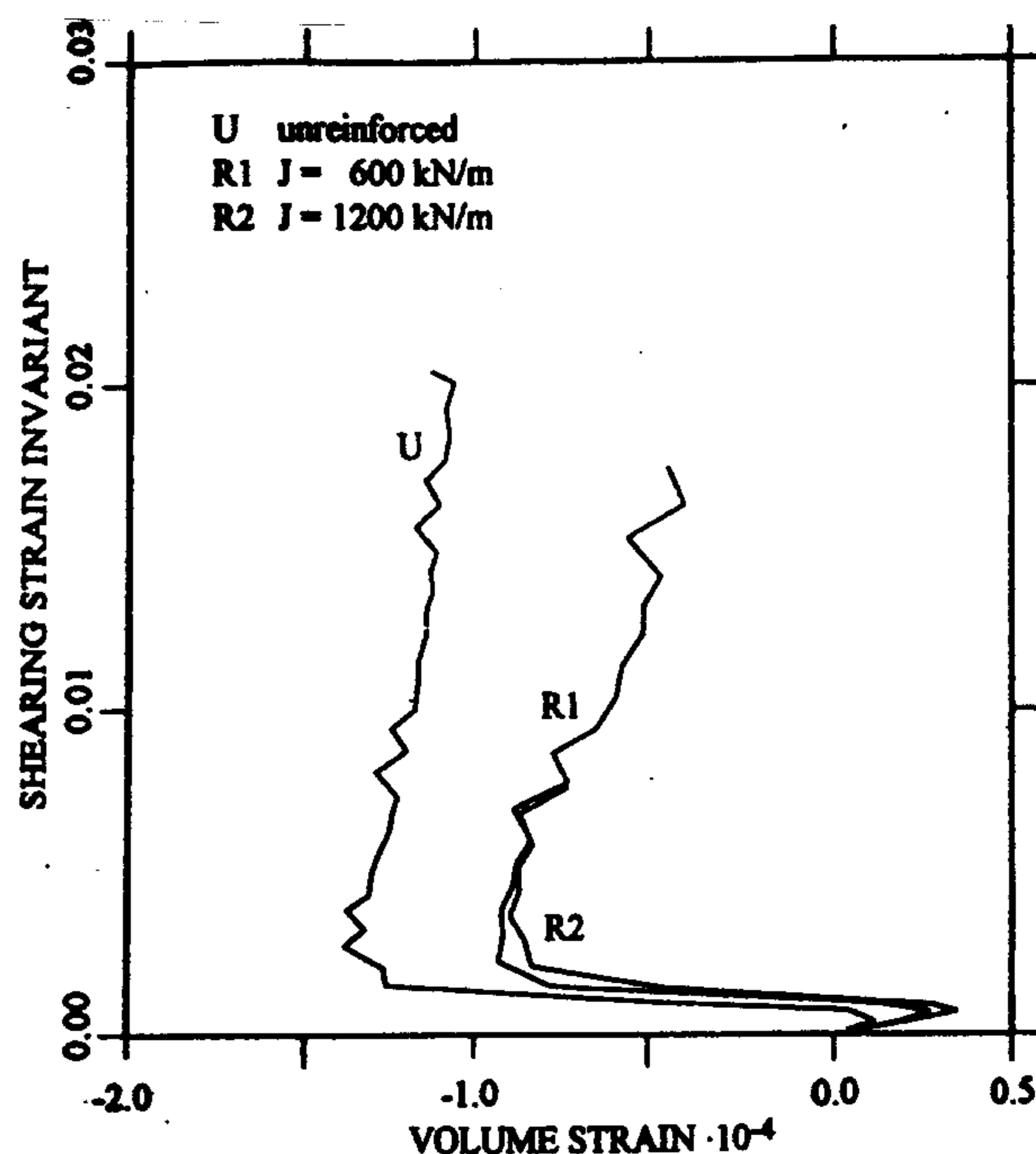


Fig. 7 Strain path of point C of foundation layer.

The reinforced road is not affected by the change in the

geosynthetic modulus at this point, but shows less horizontal stresses with respect to the unreinforced one (the strains corresponding to tension are considered negative).

The shearing strains beyond the design load is less than 17 % in the reinforced case (see fig. 8), and we can note that when geosynthetics are present, point C arrives at the failure point for values slightly higher than those for the unreinforced sample.

The failure surface relative to point C of the foundation layer is pointed out by the analysis of the stress path. We can indeed see in figure 9 the critical state line and the immediate plasticization of the foundation at this point, due to the lack of confinement caused by the presence of heavy lateral tension.

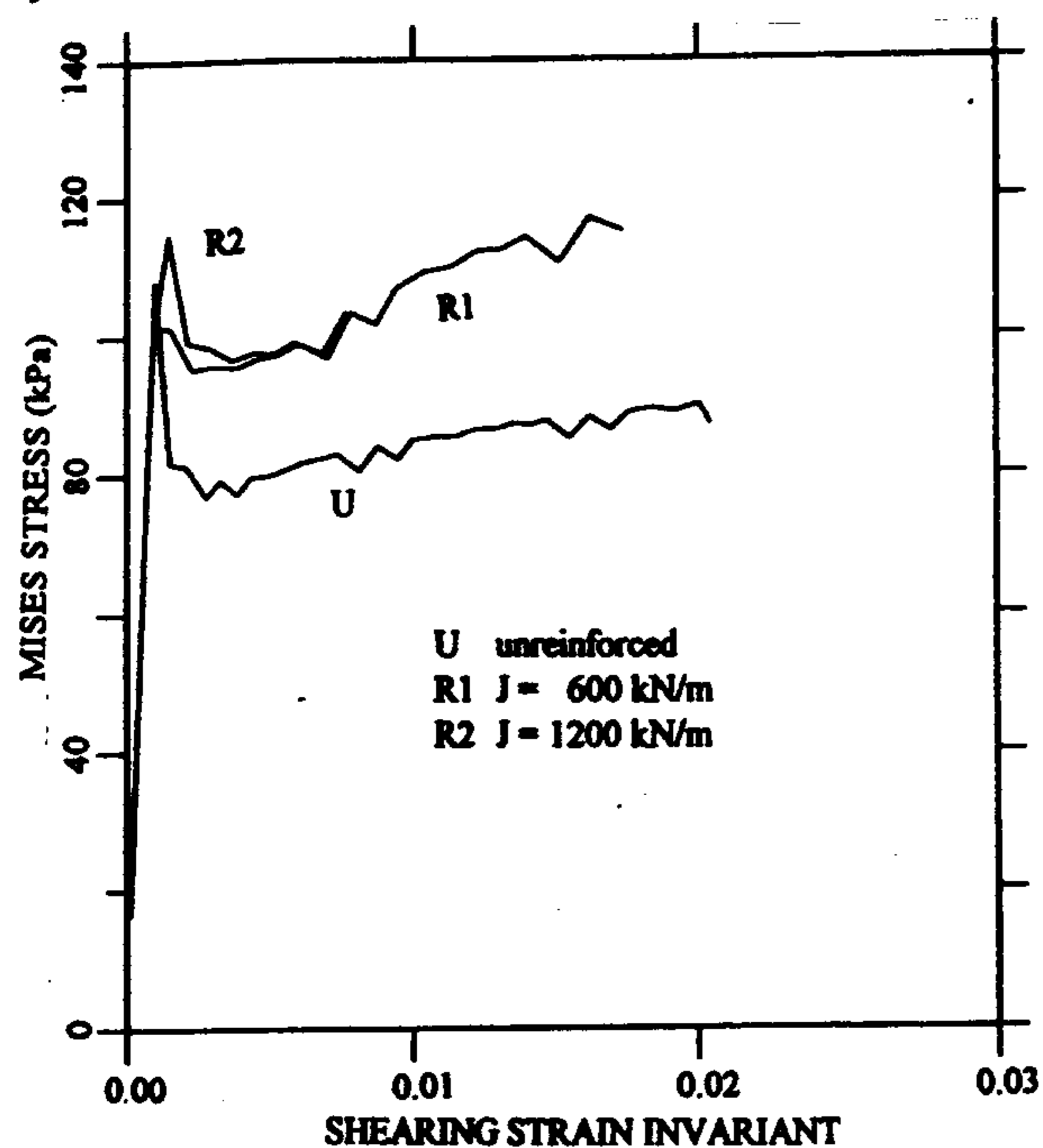


Fig. 8 Diagram relative to the variation of Mises stress vs shearing component of strains in point C.

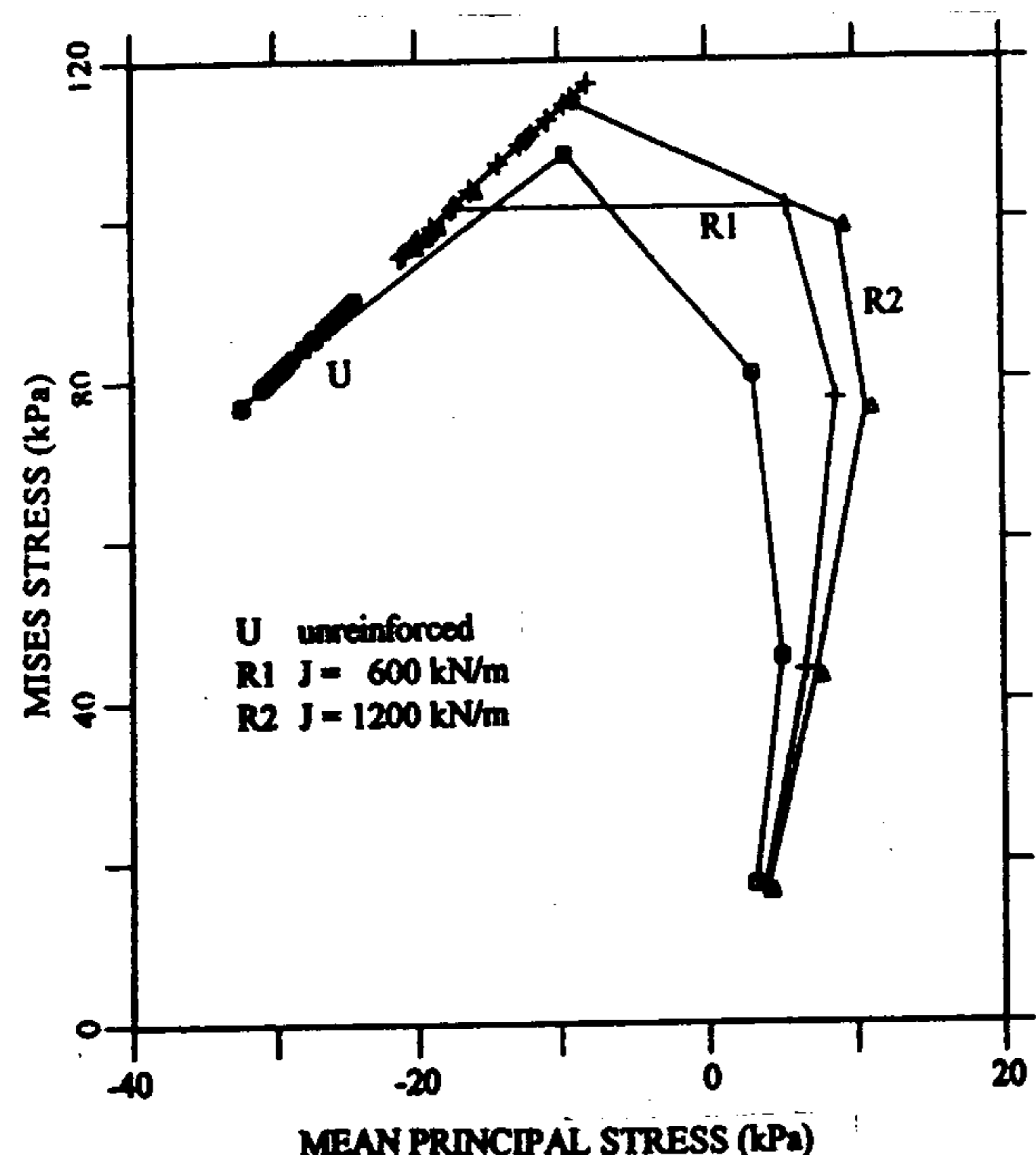


Fig. 9 Stress path relative of C zone.

Contrary to the foundation layer, the subsoil considerably benefits from the presence of the reinforcement. The strain path for point D in figure 10 shows a sharp behavioural change in the unreinforced case with respect to the reinforced one. The size of the decrease in the shearing component on the soil is -88 % for reinforcement with $J = 1200 \text{ kN/m}$, and -69 % with a modulus equal to 600 kN/m .

The modulus acts by determining a 27 % change in the features listed above, highlighting the fact that the soil behaviour is strongly affected by the latter.

This may be explained by the fact that the shear stresses, totally transmitted to the soil in the unreinforced case, are partly absorbed by the presence of the geosynthetic. Indeed, the friction coefficient between the geotextile and underlying subsoil is approximately half that of the interface between the geotextile and the granular foundation layer, which causes more freedom for relative slippage between the reinforcement and the natural soil.

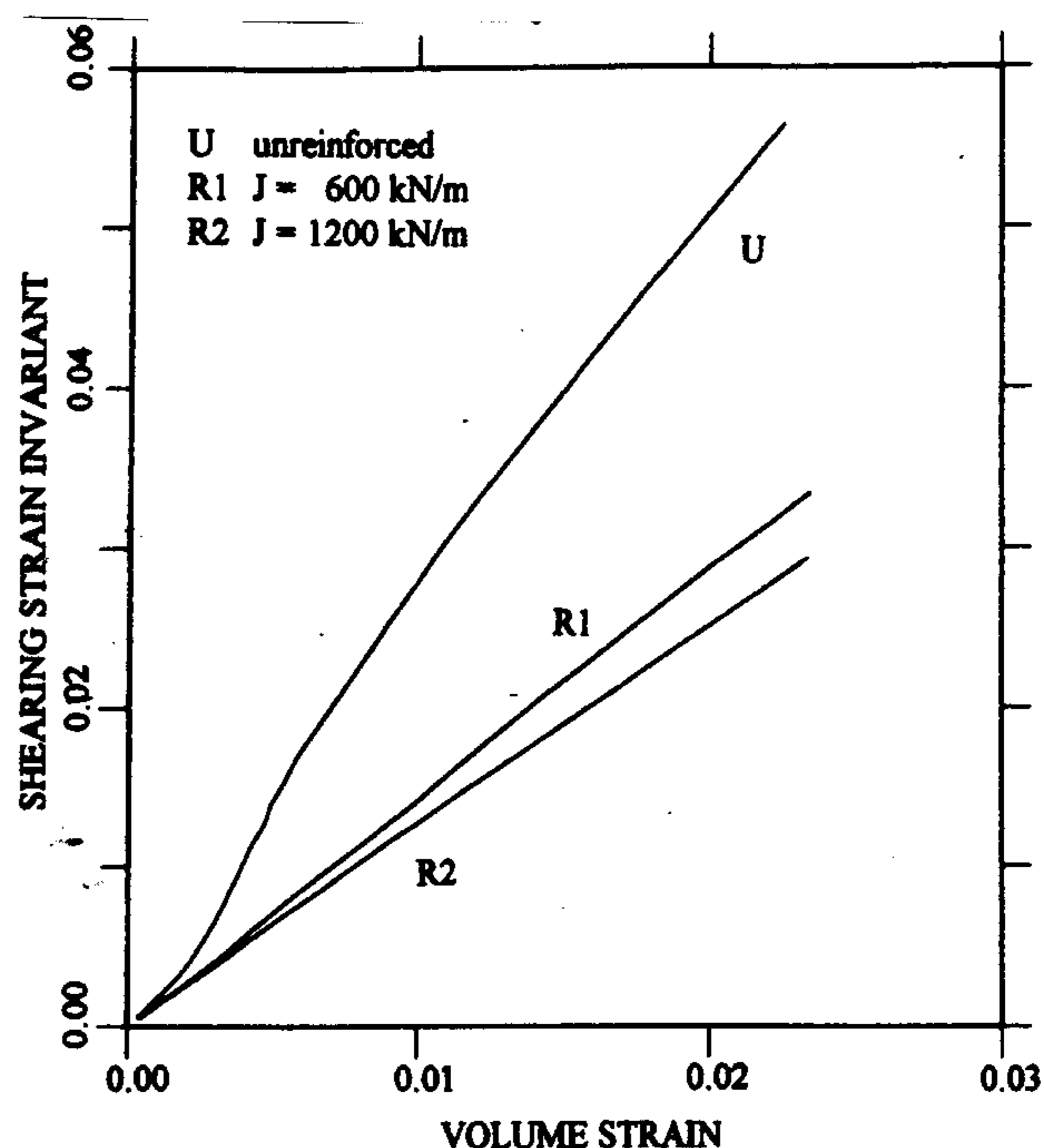


Fig. 10 Strain path relative to point D belonging to the natural underlying subsoil.

5. BEHAVIOUR OF THE PAVED ROAD IN OPERATING CONDITIONS

The analysis of the effects of inserting the reinforcement in operating conditions (130 kN axle load) highlights the increase in the performance of the paved road.

Vertical displacements decrease by approximately 20 % if the geosynthetic modulus is 1200 kN/m , and 15% if the modulus is 600 kN/m . These results are evident in figure 11, showing the percentage variation of the vertical displacements according to the distance from the loading area relative to the two reinforced cases.

The geosynthetic is not called upon to support significant

strains, the maximum Mises force / unit length arrive at values close to 5 kN/m, but in order to carry out its reinforcing role, it must ensure high stiffness to prevent excessive strain and slippage and absorb the stresses that the foundation layer would otherwise transmit to the soil. The vertical stresses do not change when the geosynthetic is present. This is understandable if we consider that the reinforcement is not stiff perpendicular to its installation plane, unless displacements arise that no longer ensure use of the paved road (membrane effect).

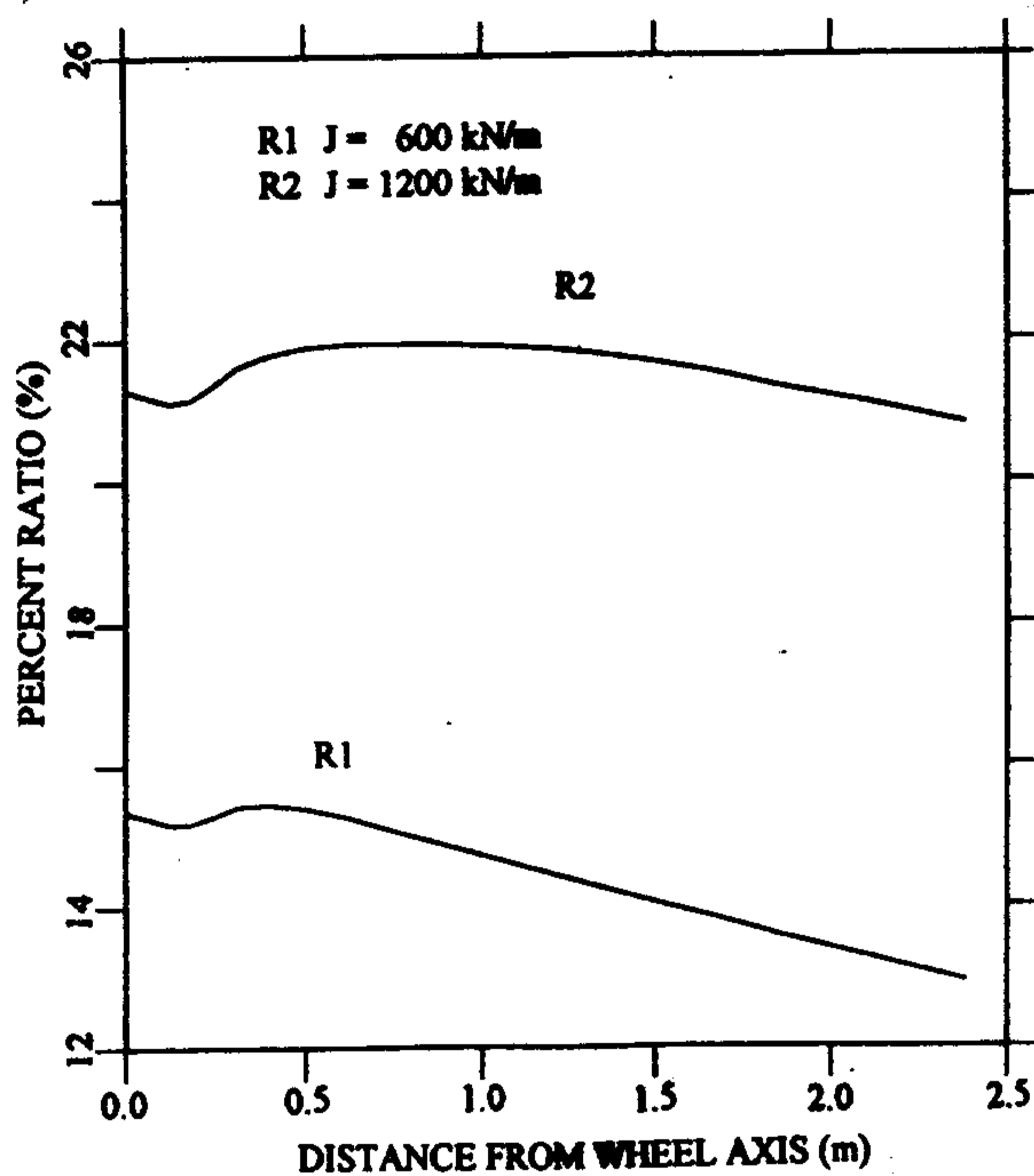


Fig. 11 Percent ratio in vertical displacements of reinforced road.

The analysis of the shearing components of strain shows that these are greater in the base area of the foundation layer, and that in the reinforced instance they take on values of less than 25%. Similarly, in the case of the volume components of strain, the presence of the reinforcement also improves distribution.

The value of the volume component of strain (1) is greater in the unreinforced than in the reinforced instance at the level of the subsoil; it should be kept in mind that the volume component of strains is the result of the sum of the three principal strains, and also the sum of the three strains in the three directions corresponding to the reference system axes.

$$\varepsilon_v = \varepsilon_{xx} + \varepsilon_{yy} + \varepsilon_{zz} \quad (1)$$

5.1 Fatigue behaviour of bituminous mixes

The analysis of the effects caused in the layer bound to bitumen due to inserting the geosynthetic was conducted taking advantage of the method used by the *Società*

Autostrade (Giannini and Camomilla, 1978).

The relation between the strain (ε_n) and the number of load cycles (N) relative to a equivalent standard axis of 130 kN is given by an expression of this type:

$$\varepsilon_N = D \cdot N^{-\alpha} \quad (2)$$

with D is the admissible strain when N=1 and depending on the composition of the bituminous mix and α an experimental coefficient that takes on a constant value equal to 0.234.

Table 2. Strains in the pavement layer in position A and B

Case	Position A		Position B	
	ε_{xx}	ε_{yy}	ε_{xx}	ε_{yy} (10^{-4})
Unreinforced	1.78	4.13	2.92	3.96
J = 600 kN/m	1.21	3.47	2.47	3.35
J = 1200 kN/m	1.05	3.28	2.33	3.16

Considering (1) both for the reinforced and unreinforced cases, it's possible to determine the percentage increase of fatigue life ($\Delta N(\%)$) in the presence of reinforcement by means of the following equation:

$$\Delta N(\%) = \left[\left(\frac{\varepsilon_u}{\varepsilon_r} \right)^{4.27} - 1 \right] \cdot 100 \quad (3)$$

In which ε_r refers to the reinforced case and ε_u to the unreinforced case. Referring to the values shown in the table 2, it is possible to determine the percentage increase of the number of load cycles referring to the reinforced cases, taking into account that we usually consider:

$$\varepsilon = \max(\varepsilon_{xx}, \varepsilon_{yy}) \quad (4)$$

the values obtained are shown in the table 3 (*).

Table 3. Increasing in fatigue life

Modulus	Increasing in fatigue life (%)
J = 600 kN/m	110.00
J = 1200 kN/m	167.50

(*) the values are relative to $\varepsilon_u = 4.13 \cdot 10^{-4}$

The table 3 show that geosynthetic insertion at the bottom of foundation layer increase the fatigue life of bituminous mixes about 2-2.5 times depending of secant modulus of reinforcement.

The fatigue check for the unbound layers is carried out considering the vertical strain (ϵ_{zz}) at point C in figure 15. The values obtained for this are: $\epsilon_{zz} = 6.3546 \cdot 10^{-3}$ in the unreinforced case; $\epsilon_{zz} = 5.2314 \cdot 10^{-3}$ in the reinforced geosynthetic case ($J = 600$ kN); $\epsilon_{zz} = 4.9369 \cdot 10^{-3}$ in the reinforced geosynthetic case ($J = 1200$ kN).

There are changes in the vertical strains of around 20 % in the case with a modulus $J = 600$ kN/m, and 28 % in the case with a modulus $J = 1200$ kN/m.

The presence of geosynthetic thus increases the life-span of the pavement; the possible load cycles are more than 2 times higher than for unreinforced structures.

The results obtained regarding the increase in the number of load cycles with the reinforcement present agree with experimental tests carried out on multilayer samples (layer bound to bitumen, granular layer and installation surface of a coherent material) subjected to cyclical load (Carrol, Walls and Haas, 1987). In this case, the reinforced samples required more than 3 times as many load cycles than the non-reinforced sample in order to achieve a rut depth of 2 cm.

5. CONCLUSIONS

In paved reinforced road analysis is of fundamental importance to consider the friction that develops within the geosynthetic/layers interface in order to have results that correspond sufficiently to the reality.

As the geosynthetic is not subject to significant vertical displacements, it acts at the base of the foundation layer, absorbing part of the shearing stresses and strains that would otherwise affect the subsoil. In this way, the subsoil must counter only vertical actions deriving from the load.

The friction that develops along the interface surface between the geosynthetic and the granular foundation layer leads to a nearly complete adherence between the two materials, contrary to what occurs in contact with the clay sub-soil, in which the relative slippage between the two surfaces is not impeded due to the low friction values which cause considerably reduced shear stresses.

It has been demonstrated that the presence of the geosynthetic makes it possible to increase the life-span of the paved road 2-2.5 times with respect to the unreinforced case, reduces vertical displacements and leads to an improved redistribution of the stresses and strains. The results achieved are strictly related to the stiffness of the geosynthetic, which compared with the modulus of subsoil, must be high and guarantee limited strains.

6. REFERENCES

- Barenberg, E.J. (1980), *Design Procedures for Soil Fabric Aggregate System with MIRAFI 500X Fabric*. University of Illinois at Urbana-Champaign.
- Barksdale, R., Robnett, Q., Lai, J. e Zeevaert-Wolff, A. (1982), *Experimental Behaviour of Geotextiles Reinforced Aggregate Soil System*. Second International Conference on Geotextiles, Las Vegas (U.S.A.).
- Burd, H.J. e Brosklehurst, C.J. (1990), *Finite Element Studies of Mechanics of Reinforced Unpaved Roads*. 4th Conference on Geotextiles, Geomembranes and Related Products, The Hague (NL).
- Carrol, R.G., Walls, J.C. e Haas R. (1987), *Granular Base Reinforcement of Flexible Pavements Using Geogrids*. Geosynthetics, New Orleans (U.S.A.).
- Chan F., Barksdale R.D. e Brown S.F. (1989), *Aggregate Base Reinforcement of Surfaced Pavements*. Geotextiles and Geomembranes, Vol. 8, pp. 165-189.
- Chinni, M. (1992), *Il rinforzo delle sovrastrutture stradali mediante geosintetici*. Degree Thesis of the Institute of Roads Construction and Geotechnics, University of Bologna (I).
- Christopher B.R. e Holtz R.D. (1991), *Geotextiles for Subgrade Stabilisation in Permanent Roads and Highways*. Geosynthetics, Atlanta.
- De Jong D.L., Peutz M.G.F. e Korswagen A.R. (1973), *Computer Program BISAR*. Koninklijke, Shell Laboratorium, Amsterdam (NL).
- Dondi G., Righi P.V. (1990), *L'utilizzo dei geosintetici nelle sovrastrutture stradali*. XXI Convegno Nazionale delle Strade, Trieste (I).
- Giannini, F. e Camomilla, G. (1978), *Progetto Strutturale delle Pavimentazioni, Impiegato per le Autostrade Italiane*. Autostrade, Vol. 2, pp. 4-17.
- Giroud, J.P., Ah-Line, C. e Bonaparte, R. (1984) *Design of Unpaved Roads and Trafficked Areas with Geogrids*. Proc. of the Symposium on Polymer Grid Reinforcement, ICE, London (U.K.).
- Giroud, J.P. e Noiray, L. (1981), *Geotextile-Reinforced Unpaved Road Design*. Journal of Geotechnical Division, ASCE, Vol. 107, N. GT9, pp. 1233-1254.
- Hausmann, M.R. (1987), *Geotextiles for Unpaved Roads, A Review of Design Procedures*. Geotextiles and Geomembranes, Vol. 5, pp. 201-233.
- Miura, N., Sakai, A. e Taesiri, Y. (1988), *Model Tests and Numerical Analysis of Reinforced Pavements by Polimer Grid*. Theory and Practice of Earth Reinforcement, Fukuoka (J).
- Sellmeijer, J.B., Kenter, C.J. e Van de Berg, C. (1982), *Calculation Method for a Fabric Reinforced Road*. Second International Conference on Geotextiles, Las Vegas (U.S.A.).